UV-blocking synthetic biopolymer from biomass-based bifuran diester and ethylene glycol

Tuomo P. Kainulainen,[a] Juho A. Sirviö,[b] Jatin Sethi,[b] Terttu I. Hukka,[c] Juha P. Heiskanen,[a]*

[a]Research Unit of Sustainable Chemistry, University of Oulu, P.O. Box 3000, FI-90014 Oulu, Finland

[b]Fibre and Particle Engineering Research Unit, University of Oulu, P.O. Box 4300, FI-90014 Oulu, Finland

[c]Laboratory of Chemistry and Bioengineering, Tampere University of Technology, P.O. Box 541, FI-33101 Tampere, Finland

Abstract

A furan-based synthetic biopolymer comprised of a bifuran monomer and ethylene glycol was synthesized through melt-polycondensation, and the resulting polyester was found to have promising thermal and mechanical properties. The bifuran monomer, dimethyl 2,2'-bifuran-5,5'-dicarboxylate, was prepared using a palladium-catalyzed, phosphine ligand-free direct coupling protocol. A titanium-catalyzed polycondensation procedure was found effective at polymerizing the bifuran monomer with ethylene glycol. The prepared bifuran polyester exhibited several intriguing properties including high tensile modulus. In addition, the bifuran monomer furnished the polyester with a relatively high glass transition temperature. Films prepared from the new polyester also had excellent oxygen and water barrier properties, which were found to be superior to those of poly(ethylene terephthalate). Moreover, the novel polyester also has good ultraviolet radiation blocking properties.

For Table of Contents Only

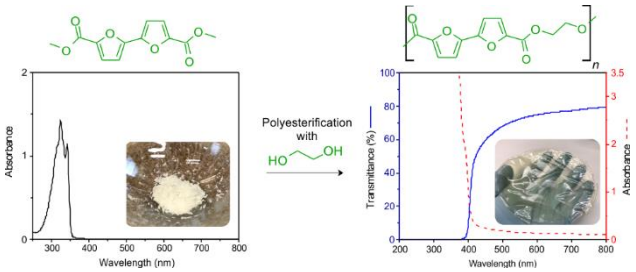

UV-blocking synthetic biopolymer from biomass-based bifuran diester and ethylene glycol

Tuomo P. Kainulainen, Juho A. Sirviö, Jatin Sethi, Terttu I. Hukka, Juha P. Heiskanen*

Introduction

Furans, which are commonly derived from C5 and C6 sugars by dehydration, form an important part of the landscape of renewable chemistry. They have been recognized as key intermediates derived from biomass.[1–3] Furfural and 5-hydroxymethyl furfural are perhaps the two best-known bio-sourced furans, and their various derivatives are useful as everything from fuels to key chemical intermediates. For these reasons, much effort has been devoted to preparing polymers from furan compounds.[4,5] Since the beginning of the last century, furans have been studied as potential precursors for polymers ranging from thermoplastics such as polyesters and polyamides to a number of thermosets. Furans also lend themselves well to thermally reversible polymerization via the Diels-Alder reaction, enabling the preparation of furan-based self-healing materials.[6]

Recently, more focused efforts have elevated 2,5-furandicarboxylic acid (2,5-FDCA, Scheme 1) into a furan building block of choice for building novel materials with great potential. Notably, this furan is the raw material of poly(ethylene furanoate) (PEF, Scheme 1). PEF is a viable alternative to poly(ethylene terephthalate) (PET, Scheme 1), a common polymer in technical plastics.[7,8] Most importantly, the gas permeability of PEF is much lower than that of PET, which is an industrially important barrier material against gases and moisture. The low permeability has been attributed to the hindered rotation and polar character of the furan ring.[9] In the future, the mainly petrochemical-based PET used for beverage and food packaging might be replaced by renewable PEF. However, combining the more commonly renewable ethylene glycol with biomass-based terephthalic acid could provide PET derived from 100% renewable resources.[10] 2,5-FDCA has also lately been used for the preparation of various other polyesters[11,12], strong aromatic polyamides[13], thermosetting epoxies[14,15], and thermoreversible self-healing materials[16], demonstrating the utility of furans as building blocks of polymers.

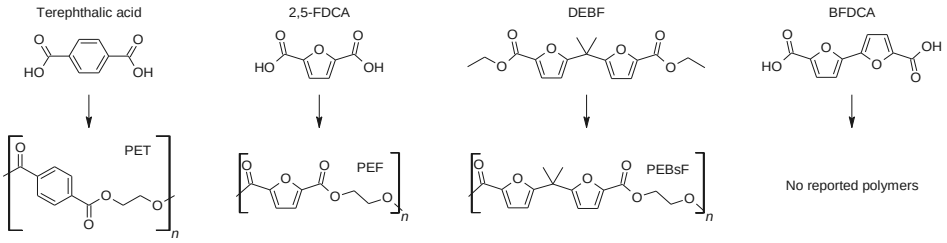

Scheme 1. The structure of PET precursor, terephthalic acid, together with the structures of some corresponding furan-based dicarboxylic acids or their ester derivatives.

However, the "dimeric" homologue of 2,5-FDCA, 2,2'-bifuran-5,5'-dicarboxylic acid (BFDCA, Scheme 1), has not received similar attention, even though its preparation was disclosed in 1966[17]. There has been some interest in utilizing bifuran moieties in organic electronics[18,19], and recently BFDCA was used to prepare coordination polymers[20] with different transition metal cations. The homologous biaryl, 4,4'-biphenyldicarboxylic acid (BDA), on the other hand, is useful for enhancing the properties of PET.[21] The co-polyesters are more suitable for high temperature, high-performance applications. Over the years, BDA has regularly appeared in patent applications related to polyesters.[22–24] It would be, therefore, intriguing to consider BFDCA as an alternative building block for various polymers in order to enhance their material properties. However, polyesters or polymers containing BFDCA have not been characterized or disclosed before, to the best of our knowledge. A related class of furan polymers prepared from the esters of "bisfuranic acids" (such as diethyl 5,5'-isopropylidene-bis(2-furoate), or DEBF, Scheme 1) is known[25,26], however their structures are fundamentally different due to the presence of a carbon spacer between the furan rings in the main chain.

In this paper, we disclose the preparation of a bifuran polyester structurally related to both PET and PEF, and present an efficient, alternative synthesis of its bifuran precursor. Due to the unique bifuran-containing structure of the polyester, it is found to have good barrier properties, i.e. low permeability to oxygen, moisture, and ultraviolet (UV) light. Typically additives in the

form of organic or inorganic absorbers are necessary to block incoming UV radiation effectively.[27] UV-protecting plastics or coatings are useful in photovoltaic cells, for example, as organic solar cells can retain more of their efficiency over time when properly protected from UV radiation.[28] The thermal and mechanical characteristics of the bifuran polyester were also found promising for future developments.

Experimental Section

Commercial solvents and reagents were used as received. Reactions were monitored using thin layer chromatography (TLC). Aluminum TLC plates with silica matrix were used with 1:1 ethyl acetate:*n*-heptane eluent. For the silica gel (Silica gel 60) filtration in the purification of compound **3**, commercial chloroform with ~0.6% of ethanol as a stabilizer was used. *N*,*N*-dimethylacetamide (DMAc) was dried over 4 Å molecular sieves.

*Synthesis of dimethyl 2,2'-bifuran-5,5'-dicarboxylate (**3**)*: Methyl 2-furancarboxylate (**1**) (6 mL, 14 equiv.), methyl 5-bromofuran-2-carboxylate (**2**) (836.8 mg, 1 equiv), potassium acetate (785.3 mg, 2 equiv.), pivalic acid (126.4 mg, 30 mol%), and palladium acetate (9.0 mg, 1 mol%) were added to a dry 50 mL round-bottom flask with a magnetic stirring bar. A reflux condenser equipped with a balloon was attached to the flask. Air inside the closed system was evacuated and replaced with argon. This was repeated five times. The reaction mixture was heated to 100 °C under stirring. After 24 h, the reaction system was cooled back to room temperature. The reaction mixture was diluted with chloroform and filtered through a silica gel plug. The silica layer was washed with chloroform until the product had been completely collected. After evaporation of chloroform under vacuum, excess starting material **1** was recovered by vacuum distillation and recycled in subsequent reactions. The dry raw product was washed by stirring it in 14 mL of hot 1:1 (v/v) mixture of chloroform and ethanol for 15 minutes. The product was recovered by vacuum filtration from cold solution, and the product was then washed with a small amount of cold ethanol. The product **3** was white to off-white

crystalline powder (876.3 mg, 88%). ^{1}H NMR (400 MHz, $CDCl_3$, ppm): δ 7.26 (d, 2H (furan), J = 3.7 Hz), 6.90 (d, 2H (furan), J = 3.7 Hz), 3.93 (s, 6H (methyl ester)). ^{13}C NMR (100 MHz, $CDCl_3$, ppm): δ 158.8 (ester carbonyl), 148.2 (furan ring), 144.3 (furan ring), 119.7 (furan ring), 109.4 (furan ring), 52.1 (ester methyl group). HRMS $[M+H]^+$: $C_{12}H_{11}O_6$, 251.0556. Found 251.0551.

Synthesis of poly(ethylene bifuranoate) (PEBF): Dimethyl 2,2'-bifuran-5,5'-dicarboxylate (**3**), ethylene glycol (5 equiv.) and tetrabutyl titanate (1 mol%) were added to a dry 50 mL round-bottom flask with a magnetic stirring bar. The flask was attached to a distillation bridge connected to argon and vacuum lines. Air inside the system was replaced with argon by evacuating the system and filling it again with argon five times. To begin the transesterification, the flask was heated to 180 °C with an aluminum heating block. Within 30 minutes, the heterogeneous mixture had turned into a pale yellow solution. The transesterification was considered complete after a total reaction time of 4 hours. At this stage, the monomer was no longer detected (TLC), and methanol ceased to distill over. Vacuum was then slowly applied to remove the excess ethylene glycol. When 3−4 mbar vacuum was reached, the temperature was increased to 270 °C. After 90 minutes, the reaction flask was allowed to cool under vacuum. The polyester was removed from the flask by dissolving it in a trifluoroacetic acid (TFA)-chloroform mixture (1:1). The polyester was then precipitated in methanol. After vacuum filtration and washing with methanol, the product was dried under vacuum to yield an off-white, fibrous material (94% yield). To prepare NMR samples, a small amount of PEBF was dissolved in TFA-d. The data (Figure 1a) conforms to the expected structure. ^{1}H NMR (400 MHz, TFA-d, ppm): δ 7.48 (d, 2H (furan), J = 3.8 Hz), 7.01 (d, 2H (furan), J = 3.8 Hz), 4.87 (s, 4H (ethylene unit)).

Dilute solution viscometry: The intrinsic viscosities were determined in trifluoroacetic acid at 30 °C using an Ostwald viscometer submerged in a thermostated water bath. From flow time

measurements (measured 10 times) for pure solvent and polymer at different concentrations, the reduced viscosities were calculated using the expression $\eta_{red} = [(t - t_0)/t_0]/c$. From a plot of η_{red} versus c, the intercept at infinite dilution was determined, and this value was taken as the intrinsic viscosity [η] (Figure S7 in Supporting Info).

ATR-FTIR: Attenuated total reflectance Fourier transform infrared spectroscopy was performed on a Perkin-Elmer Spectrum One instrument.

DSC: Differential scanning calorimeter (Mettler Toledo DSC 821e) at the temperature range of 25–300 °C with heating and cooling rates of 15 K/min under nitrogen (N_2) gas flow (60 cm^3/min) was used. The polymer samples (ca. 5 mg), were placed into 40 μL Al crucibles sealed with pierced lids.

Thermogravimetric analysis: The polymer sample (ca. 10 mg) was placed into a 70 μL Al_2O_3 crucible, which was covered with a pierced lid and placed into the thermogravimetric analyzer (Mettler-Toledo TGA851e). The sample was heated from 30 to 700 °C under nitrogen flow (95 cm^3/min) using a heating rate of 20 K/min.

Solution casting: The solution cast films were prepared by dissolving the polyester (800 mg) in TFA-chloroform mixture (2:1 v/v, 30 mL). The solution was filtered to remove any insoluble material and poured onto a Teflon petri dish (diameter 100 mm). The solvent was allowed to evaporate under reduced pressure to give a film, which was finally dried under vacuum for several days (20 °C). The formed PEBF films were almost clear with yellow hue. PET film was prepared from commercial pellets of PET (Polysciences, Inc., M_n = 20000−30000 g/mol, ^{1}H NMR in Figure S6 in Supporting Information).

Melt-pressing: Prior to melt processing, PEBF was first dried at 120 °C for 24 h, cooled, and stored in a desiccator to minimize potential degradation caused by moisture or possible solvent residues. The pressed films (Fontijne Presses LabEcon series press) were controlled to a

thickness of about 0.1 mm (tensile specimens) or 0.3 mm (gas barrier specimen) using thin metal strips as spacers. The polymer sample sandwiched between sheets of Teflon coated glass fiber mat was placed between two steel plates. The plates were heated inside the press for 3 minutes under 10 kN force at 245–255 °C. After the melting stage, the pressing force was increased to 250 kN for 1 minute. The press plates were then removed from the press and immediately quenched in cold water. To avoid warping, the 0.3 mm thick gas barrier specimen was instead quenched inside the press using the integrated water-cooling system.

Tensile testing: The films were kept under standard conditions (50% humidity, 25 °C) for 48 h and characterized with a tensile testing machine (Instron 5544, USA). Rectangular test specimens of 5 mm width were cut from films using a paper cutter. After thickness measurements (Hanatek FT3, UK), the test specimens were subjected to tensile testing using a crosshead speed of 5 mm/min with 30 mm gage length. For the stress-strain curves see Figure S9 in Supporting Information.

Dynamic mechanical analysis: The thermomechanical properties of the films were inspected by dynamic mechanical analyzer (TA Instruments DMA Q800, USA) equipped with tension (film) clamps and operating in multi-frequency mode. The rectangular specimens were prepared in the same way as for the tensile tests. Dynamic mechanical analysis at variable temperature was conducted as follows: test specimens were heated, at a rate of 5 °C /min, to 250 °C using 13 mm gap distance, 20 μm amplitude, 0.01 N preload force and 125% force track.

Gas permeability analysis: Melt-pressed films of PEBF and commercial PET were prepared as described above. The oxygen transmission rate (OTR) of the films was measured using MOCON OxTran 2/20 (Minneapolis, MN). The film was exposed to 100% oxygen gas on one side and to oxygen-free nitrogen gas on the other side. The oxygen permeability (OP) was

calculated by multiplying the OTR by the thickness of the film and dividing it by the difference in the partial pressure of the oxygen gas between the two sides of the film. The measurements were made at 23 °C, at normal atmospheric pressure, and 0% relative humidity (RH) with a specimen area of 5 cm^2. The water vapor transmission rate (WVTR) was measured using MOCON Permatran-W 3/33 (Minneapolis, MN). The film was exposed to humid nitrogen gas on one side and to dry nitrogen gas on the other side. The water vapor permeability (WVP) was calculated by multiplying the WVTR by the thickness of the film. The measurements were made at 23 °C, at normal atmospheric pressure, and 100% RH with a specimen area of 5 cm^2.

UV-Vis: A solvent cast PEBF film (thickness of 25 μm) and chloroform solution of monomer **3** (1.0 mg of compound **3** in 100 mL of chloroform, Figure S4 in Supporting Information) were measured in quartz glass cuvettes (1 cm path length) using Shimadzu UV-1800 spectrophotometer. A melt-pressed film of 50 μm thickness was used for PET due to the haziness of solvent cast films.

Powder X-ray diffraction (XRD): PXRD-measurements were taken on a PANalytical X'Pert MPD Pro using copper radiation ($K\alpha_1$ = 1.5405980 Å), equipped with an X'Celerator-detector.

Results and Discussion

In a previous paper[29], we examined the direct coupling between 5-bromofurfural and furfural. Initially our intent was to oxidize the resultant 5,5'-bisfurfural into the corresponding dicarboxylic acid. However, we found the poor solubility of 5,5'-bisfurfural problematic for purifications and further reactions. This, together with the limitations in our coupling method in terms of reaction scale had us consider alternatives.

In the past, the dimethyl ester of BFDCA, dimethyl 2,2'-bifuran-5,5'-dicarboxylate (**3**), has been synthesized through transition metal-mediated homocoupling of methyl 5-bromofuran-2-carboxylate (**2**).[17,30] The methods give the product in 68–90% yield, but they produce large

amounts of iodine and/or metal waste. Whereas, when using a more modern direct coupling approach, half of the bromide **2** can be replaced with the non-brominated methyl 2-furancarboxylate (**1**). Thus, the starting point of our new approach was the direct coupling where a similar, but asymmetric, bifuran diester was synthesized[31]. This method quickly proved promising, and it was chosen for further investigation and optimization. The results of the optimization studies are presented in Table 1.

The first experiments showed that pivalic acid (PivOH) was required for faster and more effective coupling (entries 1 and 2) in dry DMAc solvent with $Pd(OAc)_2$ as a catalyst. Of the bases tested, potassium acetate gave the highest reaction yield at the optimized reaction temperature (entries 2–7). Increasing the amount of starting material **1** from 2 to 3 and then from 3 to 4 equivalents substantially increased the yield of compound **3** (entries 3, 8, and 9, respectively), but further increasing the amount to 5 equivalents only gave a slight improvement (entry 10). When the reaction was done in the presence of excess liquid **1** (1.5 mL total, 14 equiv., entry 11) without additional organic solvent, interesting results were observed: even though the bromide was not fully spent and the reaction yield was thus lower, the reaction proceeded with minimal side-products. Simply increasing the reaction time from 4 h to 24 h finally gave the product **3** in 88% yield, fully consuming the bromide (entry 12). For these reaction conditions (Scheme 2), PivOH was found to be even more vital, as the reaction did not finish within 24 h in the absence of PivOH (entry 13). The reaction could be scaled up from the initial scale of 0.2 g of bromide **2** to up to 1.6 g of bromide **2** without much change in the reaction yields (entry 14). Furthermore, the excess starting material **1** could be effectively recovered by vacuum distillation during the purification of compound **3**. This allowed for up to 90% of the unspent reagent **1** to be salvaged. No discernible change in the reaction was observed when recycled **1** was used instead of the as-received, commercial reagent, making the overall procedure more efficient.

Table 1. Optimization of the reaction conditions for the synthesis of compound **3**.

Entry	Equiv. of **1**	Base (2 equiv.)	Temperature (°C)	Time (h)	Yield (%)
1[a]	2	KOAc	120	4	45
2	2	KOAc	120	2	50
3	2	KOAc	100	4	53
4	2	KOAc	80	24[b]	24
5	2	K_2CO_3	100	4	52
6	2	Na_2CO_3	100	24[b]	24
7	2	Cs_2CO_3	100	24[b]	-
8	3	KOAc	100	4	61
9	4	KOAc	100	4	68
10	5	KOAc	100	4	70
11[c]	14	KOAc	100	4[b]	40
12[c]	14	KOAc	100	24	88
13[a,c]	14	KOAc	100	24[b]	50[d]
14[c]	14	KOAc	100	24	87[e]

Reaction conditions: 1 equivalent of bromide **2** (0.2 g), 1 mol% of $Pd(OAc)_2$, dry DMAc (4 mL), argon atmosphere. [a]No PivOH [b]Bromide not fully consumed [c]No DMAc [d]Crude yield after silica gel filtration [e]The average yield of 10 reactions done at a scale of 1.6 g of bromide **2**.

To prepare the bifuran-*co*-ethylene glycol polyester, the simple bulk reaction between ethylene glycol and monomer **3** was chosen, as the diester could be directly used without further processing (Scheme 2). The diester may also be more widely applicable than the dicarboxylic acid, as dimethyl 2,5-furandicarboxylate has been suggested to behave more favorably under various polyesterification conditions compared to 2,5-FDCA.[32] In the first step of the polymerization, monomer **3** was transesterified with ethylene glycol in the presence of tetrabutyl titanate at 180 °C to generate intermediate **4** *in situ*. Vacuum was then gradually applied to remove the excess ethylene glycol. After reaching the final pressure of 3–4 mbar, the temperature was increased to 270 °C for 90 minutes to initiate the melt phase polycondensation of intermediate **4**, which finally yielded translucent polymer with light-brown appearance. The prepared polyester, "poly(ethylene bifuranoate)" or "PEBF", was found to be soluble in TFA and TFA-chloroform mixtures, but no solubility was observed in other tested organic solvents such as dichloromethane, chloroform, methanol, *N*-methyl pyrrolidone, or 1,1-2,2-tetrachloroethane. As TFA is highly acidic and corrosive, it could potentially degrade polyesters like PEBF. Another possibility to consider is the reaction

between TFA and the end-groups of the polyester, which in this case would cap the hydroxyl-terminated chains with TFA ester groups. Indeed, the esterification of hydroxyl end-groups occurs at room temperature in PET when it is dissolved in TFA-containing solvent, and the reaction is observable using NMR.[33] However, no degradation of the polyester chains was reported to occur under the same conditions. We did not observe any obvious degrading effects caused by TFA when working at typical room temperatures.

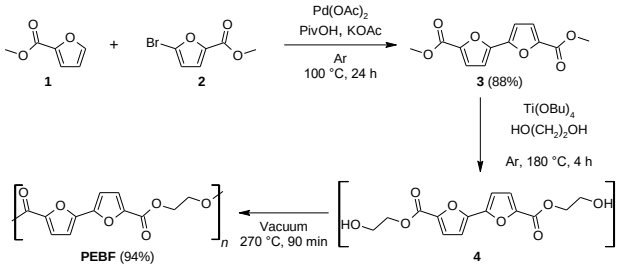

Scheme 2. The synthetic route to PEBF polyester.

NMR and FTIR analyses confirmed the expected structure of the synthesized polyester. In the ^{1}H NMR spectrum (Figure 1a), doublets corresponding to the bifuran moiety are still present, but a broad peak from the ethylene unit is seen instead of the methyl ester peak from the bifuran monomer. Furthermore, the ATR-FTIR spectrum (Figure 1b) shows absorptions associated with carbonyl groups (1718 cm^{-1}) and 2,5-substituted furan rings (1281 cm^{-1}, 1568 cm^{-1}, and 3134 cm^{-1}). Absorption at 2966 cm^{-1} corresponds to the sp^{3} carbon C-H bonds of the ethylene unit.

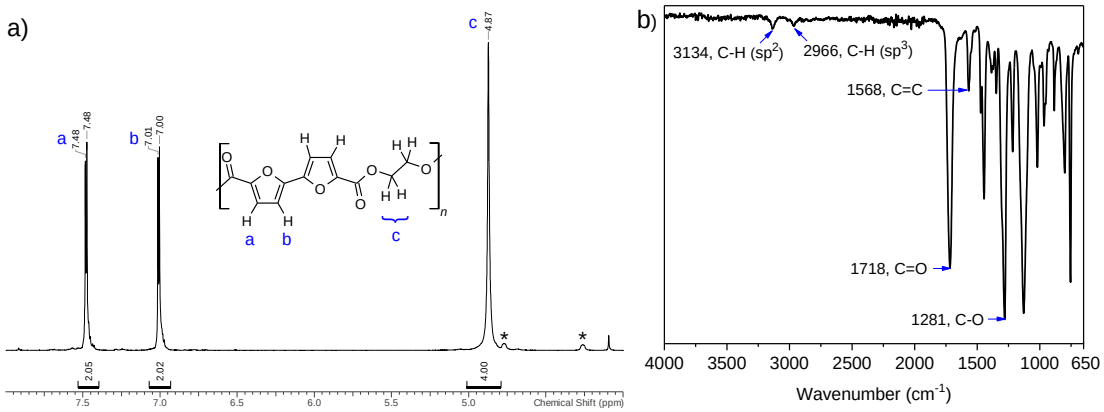

Figure 1. a) ^{1}H NMR spectrum (4–8 ppm) of PEBF polyester measured in TFA-d with the relevant peaks assigned to the repeating unit. Asterisks denote signals assigned to DEG-moieties. b) ATR-FTIR spectrum of PEBF.

Closer inspection of the ^{1}H NMR spectrum did not reveal any clear end-group signals. This suggests that the number-average molar mass (M_n) lies beyond the ten thousand range, when all polyester chains are assumed to be hydroxyalkyl-capped (see Figure S5 in Supporting Info). Additionally, two extra signals corresponding to ether and ester type -CH_2- groups are visible. This indicates the presence of diethylene glycol (DEG) units, which consist of dimerized ethylene glycol. As DEG still has two hydroxyl groups, it can easily incorporate itself into the polyester during the polycondensation. DEG is often present in different grades of PET[34], where the more flexible DEG-moieties can affect the thermal behavior of the polyester among other effects. Polyesterification between 2,5-FDCA and ethylene glycol also leads to the formation of DEG and its subsequent incorporation into PEF.[35] Based on the analysis of the ^{1}H NMR spectrum integrals, the DEG content in PEBF is estimated to be below 1% by mass (Figure S5 in Supporting Information). This is similar to the DEG content reported[35] for PEF earlier.

Dilute solution viscometry was performed for PEBF in TFA to further evaluate the formed polyesters' molar mass. At 30 °C, the intrinsic viscosity [η] was found to be 0.85 dL/g. A commercial PET sample with specified M_n=20–30 kg/mol was determined to have an intrinsic viscosity of 0.68 dL/g under the same conditions. Using the Mark–Houwink parameters of

PET[36] in TFA at 30 °C, K=0.000433 and a=0.68, the relation $[\eta] = KM_v^a$ gives viscosity average molecular weight (M_v) estimates of 70 kg/mol and 50 kg/mol for PEBF and PET, respectively. Based on the M_v value calculated for PET, the molar masses calculated appear to lie close to the expected weight-average molar masses. It should of course be noted that the values of K and a in TFA likely differ between PET and PEBF, and thus the M_v value for PEBF must include a more significant error.

According to DSC analysis (Figure 2), PEBF is a semi-crystalline polymer that has a relatively high glass transition temperature (T_g) of 107 °C (Table 2). For the sake of comparison, both PET and PEF have lower typical T_g values at 80 °C and 87 °C[37], respectively. Also, PEBF shows greatly increased glass transition temperature when compared to poly(ethylene bisfuroate) or PEBsF (T_g = 57 °C[25]). In other words, bifuran monomers with directly linked furan rings are suitable for thermally robust polymers. Despite its higher T_g, PEBF has a slightly lower melting point, T_m = 240 °C, than PET (251 °C). In this regard, PEF is the standout with its low melting point of 211 °C[37]. PEBsF, on the other hand, has not been observed to have a melting point. While the as-prepared PEBF showed a melting peak on the first heating scan, cooling at 15 K/min resulted in a practically amorphous solid, and no melting point is seen in the 2nd heating scan. PET shows clear crystallization and melting behavior under similar conditions (Figure S8).

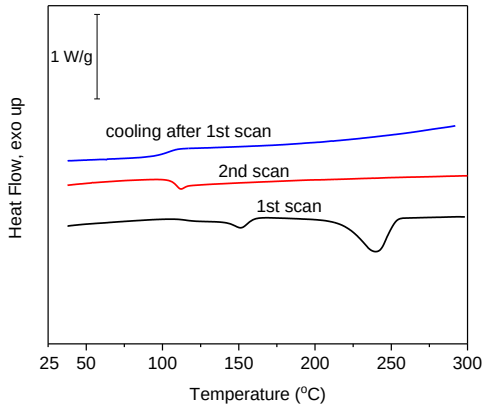

Figure 2. The DSC trace of PEBF measured under nitrogen gas.

Figure 3 depicts the TGA traces of PET and PEBF between 200 and 700 °C under nitrogen atmosphere, where both polyesters decomposed in a single step. For PEBF, 5% weight loss (T_{d5}) was observed at 397 °C, and the weight loss rate reached a maximum (T_d) at 429 °C. For PET, T_{d5} and T_d were both higher at 420 °C and 458 °C, respectively. After the TGA runs, about 25% of the initial sample weight was left as a residue for PEBF, while only 15% was left of the PET sample. These values appear to be in agreement with the higher content of aromatic units in PEBF. Based on the thermogravimetric analysis, PEBF has thermal weight loss characteristics quite similar to PET and PEF, though the decomposition temperatures are slightly lower than for PET. The thermal weight loss in PEBF is quite comparable to furan-based PEF[38], which seems reasonable considering they have similar furan ester linkages.

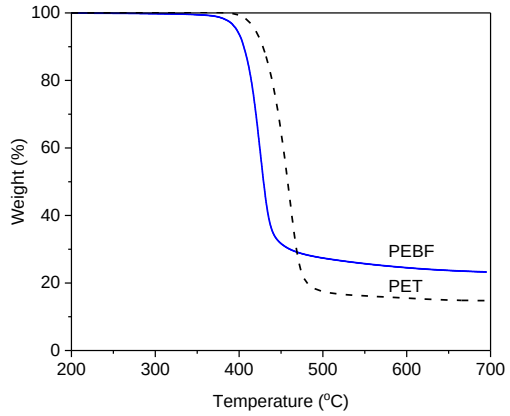

Figure 3. The TGA traces of PEBF and PET measured under nitrogen atmosphere.

Table 2. Thermal properties of PEBF compared to other polyesters prepared with ethylene glycol.

Polyester	T_g (°C)	T_c (°C)	T_m (°C)	T_{d5} (°C)	T_d (°C)
PEBF	107	169	240	397	429
PET	80	172[ref 37]	251	420	458
PEF	87[ref 37]	-	211[ref 37]	-	-
PEBsF	57[ref 25]	-	-	-	-

T_g: glass transition temperature, 2nd heating. T_c: crystallization temperature. T_m: melting temperature, 1st heating. T_{d5}: temperature at 5% weight loss. T_d: temperature at maximum weight loss rate.

Since furan-based PEF has proven to be superior to PET in terms of its gas barrier properties, it was expected that bifuran-based PEBF would have lower gas permeability than PET. Barrier properties of PEBF were probed by measuring the oxygen and water vapor permeability of melt-pressed films, and the results were compared to a PET specimen (Table 3). As expected, the PEBF film was much less permeable to oxygen and moisture than the PET film, and for both permeants, approximately two-fold decrease in permeability was observed. The permeability of the PET film was also in good agreement with previous studies, where its oxygen permeability has been compared to PEF.[39] Overall, the oxygen and water permeability values of PEBF place it between PET and PEF in terms of barrier performance.

Table 3. Gas permeability and barrier improvement factor (BIF) of melt-pressed, unoriented PEBF compared to PET.

Polyester	Oxygen permeability[a]		Water vapor permeability[b]	
	Permeability (barrer)	BIF	Permeability (g μm m^{-2} day^{-1})	BIF
PEBF	0.041	2.4	346.469	1.8
PET	0.099	1.0	616.711	1.0

[a]Oxygen permeability at 23 °C, normal atmospheric pressure, 0% RH [b]Water vapor permeability at 23 °C, normal atmospheric pressure, 100% RH.

Another barrier property considered was the UV-light permeability, where a change was anticipated due to the extended conjugation in the employed diacid monomer. The effect of the bifuran unit on the UV-properties of the polyester was evaluated via UV-Vis measurements (Figure 4). A thin, solvent cast PEBF film displayed excellent UV-blocking ability all the way up to the UV-A range of 315–400 nm, where most of the UV-radiation intensity at Earth's surface falls within. The observed result is a direct consequence of the bifuran structure, which

contains a conjugation system long enough to give monomer **3** good absorption in the UV-A range.

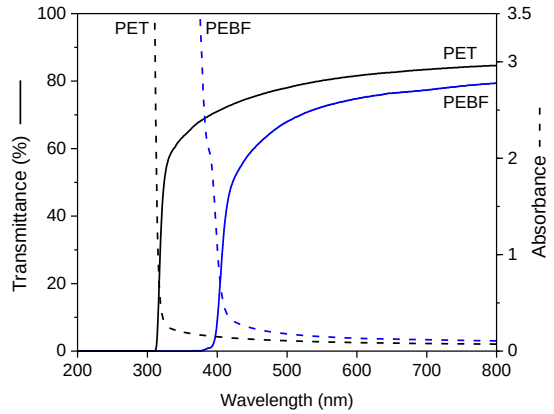

Figure 4. UV-Vis absorption and transmittance of a PEBF film (thickness 25 μm) and a PET film.

In addition, the transmittance of the PEBF film between 420–800 nm was up to 80%, which matched the good visual transparency of the film. However, the absorptivity of the PEBF film slightly tailed into the visible wavelengths, giving the film a light yellow tint (Figure 5). While monomer **3** exhibits good absorption at UV-wavelengths, it does not show any absorption near visible wavelengths (Figure S4 in Supporting Information). This leads us to conclude that unknown impurities formed in small amounts during the synthesis of PEBF are the probable main cause of the observed discoloration. Exposure to relatively harsh conditions, such as those we used to prepare PEBF, are known to discolor PET and PEF in similar fashion.[38,40] However, due to the high melting point of PEBF, high temperatures are difficult to avoid during polymerization.

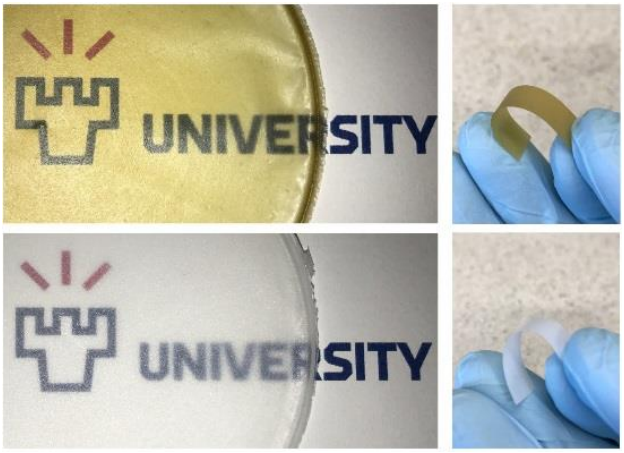

Figure 5. Pictures of PEBF (top) and PET (bottom) films and cut strips demonstrating the flexibility and the visual appearance of the solvent cast films.

To gain further understanding of the material properties of the novel bifuran polyester, test specimens cut from solution cast films of both PEBF and commercial PET were subjected to tensile testing (Table 4). Both of the flexible, freestanding films were prepared using the same protocol. In our testing, the solvent cast PEBF film consistently performed better than the PET film, with average tensile modulus and maximum tensile stress values 25% and 40% higher, respectively. The elongation at break values for both materials were relatively low at below 5%, which indicates brittle character. The melt pressed PEBF film was even more brittle, as evidenced by the lowered elongation at break (Table 4). The melt-pressed PET was much more ductile. Thus, even though the PEBF specimens had over 50% higher tensile modulus than PET specimens, the tensile strength became low due to the lack of elongation. From our comparative test, it can be concluded that the prepared PEBF had reached high molar mass, and was able to challenge PET under similar circumstances in terms of mechanical performance. Though the mechanical values for PET are somewhat different than those found[37,41,42] in various comparisons, differences in molar masses, additives, thermal histories, orientation, and testing make comparison between reported values difficult.

Table 4. The mechanical performance of solvent cast and melt-pressed PEBF and PET films.

Polyester	Solvent cast			Melt-pressed		
	E_t (MPa)	σ_m (MPa)	ε_b (%)	E_t (MPa)	σ_m (MPa)	ε_b (%)
PEBF	1182±149	23.0±2.7	4.50±0.97	2453±140	12±1	0.50±0.05
PET	948±60	16.1±1.5	3.74±0.37	1622±51	35±6	20.05±7.04

E_t: Tensile modulus. σ_m: Ultimate tensile strength. ε_b: Elongation at break. For stress-strain curves, see Figure S9 in Supporting Information.

Dynamic mechanical analysis (Figure 6) performed on the melt-pressed PEBF film further supported the findings from the thermal experiments: tan δ reaches its peak value at 108 °C, signaling the transition from glassy state to rubbery state. From the loss modulus (E'') curve, on the other hand, a glass transition temperature of 99 °C is found. Furthermore, storage modulus (E') starts to increase after 140 °C, which is consistent with cold crystallization.

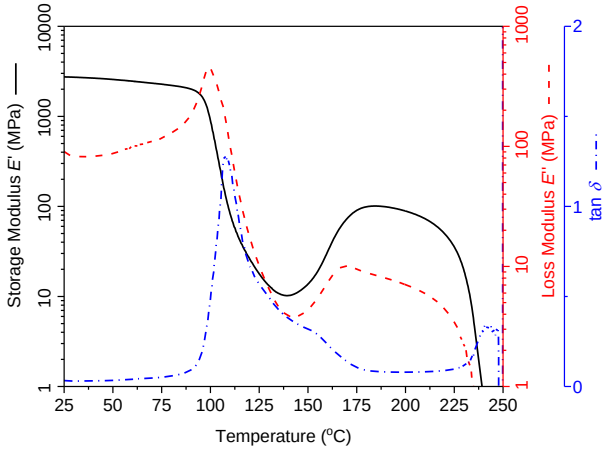

Figure 6. Storage modulus (E'), loss modulus (E''), and tan δ of PEBF as functions of temperature.

The polyester films were also characterized using X-ray powder diffraction (XRD). Figure 7 shows the XRD patterns of PET and PEBF obtained from the solvent cast films. The PET film is much more crystalline, and shows prominent peaks at 16.7° and 25.9° that correspond to distances of 5.30 Å and 3.49 Å (Figure 7b). The shorter spacing most likely corresponds to π-π-stacking of individual polymer chains, while the origin of the peak at 16.7° could not be discerned. The PEBF, on the other hand, appears clearly much more amorphous (Figure 7a).

Only a broad “halo” is resolved between 15 and 30°, along with a possible weak reflection at 16.7°. This would suggest that PEBF does not crystallize from solution as easily as PET.

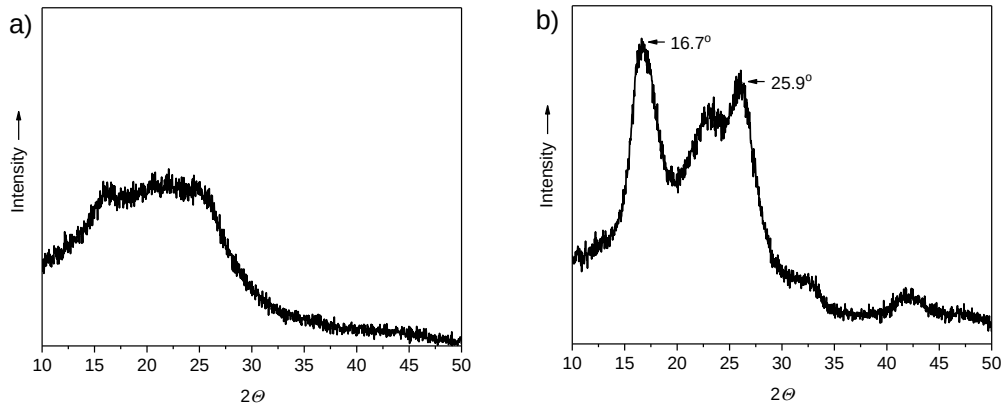

Figure 7. XRD patterns measured from a) PEBF and b) PET obtained from solvent cast films.

Conclusions

The synthesis of biomass-based bifuran monomer **3** was studied and optimized. Unlike in the previous methods found in the literature, a high yield is achieved using a direct coupling method. Furthermore, utilization of a non-brominated coupling partner is a step towards a more green synthesis of the potentially useful bifuran monomer **3**.

Most importantly, monomer **3** undergoes a condensation reaction with ethylene glycol to yield a mechanically strong, if brittle, polyester PEBF. Due to its main components, its final structure can include carbon exclusively derived from biomass. Based on measured barrier properties, it appears that substituting the phenyl rings of PET with bifuran structure notably decreases the permeability to both water vapor and oxygen. PEBF also acts as a UV-blocking material, which is explained by the conjugated bifuran ring system shifting the absorption of the final polyester. In terms of thermal properties the observed values were satisfactory, with high T_g of 107 °C and decomposition temperatures in the range of 400 °C.

The observed barrier properties of PEBF would make bifuran-based materials promising for various packaging and substrate applications where the observed barrier behavior might be

desired. After all, many traditional plastics by themselves, such as PET[43], are mostly transparent at UV-A wavelength. We envision that PEBF, or other co-polymers of **3**, could be useful for enhancing and modifying the mechanical, thermal, or barrier characteristics of materials in green manner.

Associated content

Supporting Information: ^{1}H and ^{13}C NMR spectra for compound **3** (Figures S1 and S2, respectively), HRMS data for compound **3** (Figure S3), UV-Vis data for compound **3** (Figure S4), ^{1}H NMR spectra for PEBF (Figure S5) and commercial PET (Figure S6), plots of reduced viscosity versus concentration in TFA for PEBF and PET (Figure 7), DSC trace of commercial PET (Figure S8), stress-strain curves measured from PEBF and PET specimens (Figure S9), DMA thermogram (PET) (Figure S10).

Author Information

*Corresponding Author: Juha P. Heiskanen. E-mail: juha.heiskanen@oulu.fi

Author Contributions: The manuscript was written through contributions of all authors. All authors have given approval to the final version of the manuscript.

Notes: The authors declare no competing financial interest.

We thank Päivi Joensuu and Henrik Romar for providing HRMS and ATR-FTIR data, respectively. We also gratefully acknowledge Frank Pammer for providing the XRD data. Dr. Petteri Piltonen is acknowledged from help with DMA measurement. The authors acknowledge the EU/European Regional Development Fund, Leverage from the EU program (project number A71029) for financial support. Alfred Kordelin Foundation and Magnus Ehrnrooth Foundation are acknowledged for funding of the project.

References

(1) Gandini, A., Lacerda, T. M., Carvalho, A. J. F., Trovatti, E. Progress of Polymers from Renewable Resources: Furans, Vegetable Oils, and Polysaccharides. *Chem. Rev.* **2016**, *116*, 1637–1669.

(2) Bohre, A., Dutta, S., Saha, B., Abu-Omar, M. M. Upgrading Furfurals to Drop-in Biofuels: An Overview. *ACS Sustainable Chem. Eng*. **2015**, *3*, 1263−1277.

(3) Corma, A., Iborra, S., Velty, A. Chemical Routes for the Transformation of Biomass into Chemicals. *Chem. Rev.* **2007**, *107*, 2411−2502.

(4) Moreau, C., Belgacem, M. N., Gandini, A. Recent catalytic advances in the chemistry of substituted furans from carbohydrates and in the ensuing polymers. *Top. Catal.* **2004**, *27*, 11–30.

(5) Gandini, A., Belgacem, M. N. Furans in polymer chemistry. *Prog. Polym. Sci.* **1997**, *22*, 1203−1379.

(6) Gandini, A. The furan/maleimide Diels–Alder reaction: A versatile click–unclick tool in macromolecular synthesis. *Prog. Polym. Sci.* **2013**, *38*, 1–29.

(7) Sousa, A. F., Vilela, C., Fonseca, A. C., Matos, M., Freire, C. S. R., Gruter, G.-J. M., Coelho, J. F. J., Silvestre, A. J. D. Biobased polyesters and other polymers from 2,5-furandicarboxylic acid: a tribute to furan excellency. *Polym. Chem.* **2015**, *6*, 5961−5983.

(8) Gandini, A., Silvestre, A. J. D., Neto, C. P., Sousa, A. F., Gomes, M. The Furan Counterpart of Poly(ethylene terephthalate): An Alternative Material Based on Renewable Resources. *J. Polym. Sci., Part A: Polym. Chem.* **2009**, *47*, 295−298.

(9) Burgess, S. K., Kriegel, R. M., Koros, W. J. Carbon Dioxide Sorption and Transport in Amorphous Poly(ethylene furanoate). *Macromolecules* **2015**, *48*, 2184−2193.

(10) Pang, J., Zheng, M., Sun, R., Wang, A., Wang, X., Zhang, T. Synthesis of ethylene glycol and terephthalic acid from biomass for producing PET. *Green Chem.* **2016**, *18*, 342–359.

(11) Zhu, J., Cai, J., Xie, W., Chen, P.-H., Gazzano, M., Scandola, M., Gross, R. A. Poly(butylene 2,5-furan dicarboxylate), a Biobased Alternative to PBT: Synthesis, Physical Properties, and Crystal Structure. *Macromolecules* **2013**, *46*, 796–804.

(12) Jiang, M., Liu, Q., Zhang, Q., Ye, C., Zhou, G. A Series of Furan-Aromatic Polyesters Synthesized via Direct Esterification Method Based on Renewable Resources. *J. Polym. Sci., Part A: Polym. Chem.* **2012**, *50*, 1026–1036.

(13) Luo, K., Wang, Y., Yu, J., Zhu, J., Hu, Z. Semi-bio-based aromatic polyamides from 2,5-furandicarboxylic acid: toward high-performance polymers from renewable resources. *RSC Adv.* **2016**, *6*, 87013−87020.

(14) Miao, J.-T., Yuan, L., Guan, Q., Liang, G., Gu, A. Biobased Heat Resistant Epoxy Resin with Extremely High Biomass Content from 2,5-Furandicarboxylic Acid and Eugenol. *ACS Sustainable Chem. Eng.* **2017**, *5*, 7003−7011.

(15) Deng, J., Liu, X., Li, C., Jiang, Y., Zhu, J. Synthesis and properties of a bio-based epoxy resin from 2,5-furandicarboxylic acid (FDCA). *RSC Adv.* **2015**, *5*, 15930−15939.

(16) Ryu, Y. S., Oh, K. W., Kim, S. H. Synthesis and Characterization of a Furan-Based Self-Healing Polymer. *Macromol. Res.* **2016**, *24*, 874−880.

(17) Grigg, R., Knight, J. A., Sargent, M. V. Studies in Furan Chemistry. Part IV. 2,2'-Bifurans. *J. Chem. Soc. C* **1966**, *0*, 976−981.

(18) Matsidik, R., Luzio, A., Askin, Ö., Fazzi, D., Sepe, A., Steiner, U., Komber, H., Caironi, M., Sommer, M. Highly Planarized Naphthalene Diimide−Bifuran Copolymers with Unexpected Charge Transport Performance. *Chem. Mater.* **2017**, *29*, 5473−5483.

(19) Gidron, O., Varsano, N., Shimon, L. J. W., Leitus, G., Bendikov, M. Study of a bifuran vs. bithiophene unit for the rational design of p-conjugated systems. What have we learned? *Chem. Comm.* **2013**, *49*, 6256−6258.

(20) Huang, X., Chen, D., He, M., Li, J., Huang, J., Li, B. Crystal structure and luminescent properties of novel coordination polymers constructed with bifurandicarboxylic acid. *Acta Cryst.* **2017**, *73*, 715−721.

(21) Asrar, J. Synthesis and Properties of 4,4'-Biphenyldicarboxylic Acid and 2,6-Naphthalenedicarboxylic Acid. *J. Polym. Sci., Part A: Polym. Chem.* **1999**, *37*, 3139−3146.

(22) Liu, H., Mondschein, R. J., Chen, T., Long, T. E., Turner, R. S. Terephthalate-co-bibenzoate polyesters. PCT Int. Appl. WO2017112031 (A1), 2017.

(23) Delker, R. High-strength core-sheath polyester monofilaments and their manufacture and industrial uses. Eur. Pat. Appl. EP735165 (A2), 1996.

(24) Choe, E. W., Flint, J. A. Copolyesters for high-modulus fibers. PCT Int. Appl. WO9302122 (A1), 1993.

(25) Bougarech, A., Abid, M., Abid, S., Fleury, E. Synthesis, characterization and thermal, hydrolytic and oxidative degradation study of biobased (BisFuranic-Pyridinic) copolyesters. *Polym. Degrad. Stab.* **2016**, *133*, 283–292.

(26) Khrouf, A., Abid, M., Boufi, S., El Gharbi, R., Gandini, A. Polyesters bearing furan moieties, 2. A detailed investigation of the polytransesterification of difuranic diesters with different diols. *Macromol. Chem. Phys.* **1998**, *199*, 2755–2765.

(27) Murphy, J. Modifying Specific Properties: Resistance to Light - UV Stabilizers. *Additives for Plastics Handbook*, 2nd ed.; Elsevier: Kidlington, Oxford, UK, 2001; pp 107−114.

(28) Bella, F., Griffini, G., Gerosa, M., Turri, S., Bongiovanni, R. Performance and stability improvements for dye-sensitized solar cells in the presence of luminescent coatings. *J. Power Sources* **2015**, *283*, 195−203.

(29) Kainulainen, T. P., Heiskanen, J. P. Palladium catalyzed direct coupling of 5-bromo-2-furaldehyde with furfural and thiophene derivatives. *Tetrahedron Lett.* **2016**, *57*, 5012–5016.

(30) Takagi, K., Hayama, N., Sasaki, K. Ni(0)-Trialkylphosphine Complexes. Efficient Homo-coupling Catalyst for Aryl, Alkenyl, and Heteroaromatic Halides. *Bull. Chem. Soc. Jpn.* **1984**, *57*, 1887–1890.

(31) Fu, H. Y., Zhao, L., Bruneau, C., Doucet, H. Palladium-Catalysed Direct Heteroarylations of Heteroaromatics Using Esters as Blocking Groups at C2 of Bromofuran and Bromothiophene Derivatives: A One-Step Access to Biheteroaryls. *Synlett* **2012**, *23*, 2077−2082.

(32) Tsanaktsis, V., Papageorgiou, G. Z., Bikiaris, D. N. A Facile Method to Synthesize High-Molecular-Weight Biobased Polyesters from 2,5-Furandicarboxylic Acid and Long-Chain Diols. *J. Polym. Sci., Part A: Polym. Chem.* **2015**, *53*, 2617−2632.

(33) Kenwright, A. M., Peace, S. K., Richards, R. W., Bunn, A., MacDonald, W. A. End group modification in poly(ethylene terephthalate). *Polymer* **1999**, *40*, 2035–2040.

(34) Martínez de Ilarduya, A., Muñoz-Guerra, S. Chemical Structure and Microstructure of Poly(alkylene terephthalate)s, their Copolyesters, and their Blends as Studied by NMR. *Macromol. Chem. Phys.* **2014**, *215*, 2138−2160.

(35) Thiyagarajan, S., Vogelzang, W., Knoop, R. J. I., Frissen, A. E., van Haveren, J., van Es, D. S. Biobased furandicarboxylic acids (FDCAs): effects of isomeric substitution on polyester synthesis and properties. *Green Chem.* **2014**, *16*, 1957−1966.

(36) Wallach, M. L. Mark-Houwink relation and unperturbed dimensions of poly(ethylene terephthalate). *Polym. Prepr. (Am. Chem. Soc., Div. Polym. Chem.)* **1965**, *6*, 860–867.

(37) Hong, S., Min, K.-D., Nam, B.-U., Park, O. O. High molecular weight bio furan-based co-polyesters for food packaging applications: synthesis, characterization and solid-state polymerization. *Green Chem.* **2016**, *18*, 5142−5150.

(38) Terzopoulou, Z., Karakatsianopoulou, E., Kasmi, N., Majdoub, M., Papageorgiou, G. Z., Bikiaris, D. N. Effect of catalyst type on recyclability and decomposition mechanism of poly(ethylene furanoate) biobased polyester. *J. Anal. Appl. Pyrolysis* **2017**, *106*, 357−370.

(39) Burgess, S. K., Karvan, O., Johnson, J. R., Kriegel, R. M., Koros, W. J. Oxygen sorption and transport in amorphous poly(ethylene furanoate). *Polymer* **2014**, *55*, 4748–4756.

(40) Yang, J., Xia, Z., Kong, F., Ma, X. The effect of metal catalyst on the discoloration of poly(ethylene terephthalate) in thermo-oxidative degradation. *Polym. Degrad. Stab.* **2010**, *95*, 53−58.

(41) Knoop, R. J. I., Vogelzang, W., van Haveren, J., van Es, D. S. High Molecular Weight Poly(ethylene-2,5-furanoate); Critical Aspects in Synthesis and Mechanical Property Determination. *J. Polym. Sci., Part A: Polym. Chem.* **2013**, *51*, 4191−4199.

(42) Yu, Z., Zhou, J., Cao, F., Zhang, Q., Huang, K., Wei, P. Synthesis, Characterization and Thermal Properties of Bio-Based Poly(Ethylene 2,5-Furan Dicarboxylate). *J. Macromol. Sci., Part B: Phys.* **2016**, *55*, 1135−1145.

(43) Hess, S. C., Permatasari, F. A., Fukazawa, H., Schneider, E. M., Balgis, R., Ogi, T., Okuyama, K., Stark, W. J. Direct synthesis of carbon quantum dots in aqueous polymer solution: one-pot reaction and preparation of transparent UV-blocking films. *J. Mater. Chem. A* **2017**, *5*, 5187−5194.